THE JOURNAL OF PROSTHETIC DENTISTRY

RESEARCH AND EDUCATION

Optimal design of the retainer and connector for a lithium disilicate resin-bonded fixed partial denture: A finite element analysis study

Yujia Liu, MDS,[a] Yijia Huang, BDS,[b] Sijing Chu, BDS,[c] Qiangqiang Fu, MS,[d] Haixia Liu, PhD,[e] Fan He, BDS,[f] and Yuhua Wang, DDS, PhD[g]

ABSTRACT

Statement of problem. How the connector shape, retainer type, and retainer placement affect the functional stresses in lithium disilicate cantilever resin-bonded fixed partial dentures (RBFPDs) is unclear.

Purpose. The purpose of this finite element analysis (FEA) study was to evaluate the effects of the connector shape, retainer type, and retainer placement on the stress distribution and magnitude of stress in RBFPDs.

Material and methods. Cantilever RBFPDs of the maxillary anterior lateral incisor with a retainer on the canine were modeled to conduct a 3-dimensional FEA. These designs were divided into 2 groups based on connector shape: rectangular and trapezoidal. Each group included 4 different retainer configurations—either labial or palatal veneer RBFPDs (LV-RBFPD or PV-RBFPD) or labial or palatal contact-point RBFPDs (LC-RBFPD or PC-RBFPD). FEA was performed for each RBFPD to evaluate stresses during regional and 3-point loading, including maximal intercuspal, protrusive, and lateral mandibular positions. The results were evaluated via colorimetric stress maps of the equivalent von Mises stress, maximum principal stress, and minimum principal stress in the prosthesis.

Results. The connector shape, retainer type, and placement affected the RBFPD stress, and the lowest stress was observed in the rectangular group. The LC-RBFPD group presented the lowest maximum principal stress (348.2 MPa) and minimum principal stress (49.1 MPa) under regional loading and the lowest equivalent stress (273.4 MPa) and maximum principal stress (356.0 MPa) with the protrusion position. The LV-RBFPD group presented the lowest equivalent stress (52.0 MPa), the lowest maximum principal stress (47.5 MPa), and the minimum principal stress (1.04 MPa) at the maximal intercuspal position, the lowest minimum principal stress (1.04 MPa) at the protrusion position, and the lowest equivalent stress (46.7 MPa) at the lateral position. The PV-RBFPD group presented the lowest equivalent stress (268.5 MPa) under regional loading and the lowest maximum principal stress (37.7 MPa) and minimum principal stress (2.02 MPa) under lateral loading.

Conclusions. A rectangular cross-sectional connector design for all groups could help disperse occlusal force and improve the resistance of the restoration. Both the veneer and contact-point retainer in the rectangular group were clinically acceptable and could resist fracture. (J Prosthet Dent xxxx;xxx:xxx-xxx)

Supported by the Science and Technology Committee of Yangpu District, Shanghai, PR China (grant no. YPQ202403); the Science and Technology Committee of Fengxian District, Shanghai, PR China (grant no. FK20221402); the National Clinical Research Center for Oral Diseases, Shanghai, PR China (grant no. NCRCO202332); and the Shanghai Natural Science Foundation (grant no. 24ZR1443600), PR China.
The authors declare no conflict of interest.

[a]Dental Attending, Department of Stomatology, Yangpu Hospital, School of Medicine, Tongji University, Shanghai, PR China.
[b]Graduate student, Department of Prosthodontics, Shanghai Ninth People's Hospital, Shanghai Jiao Tong University School of Medicine; College of Stomatology, Shanghai Jiao Tong University; National Center for Stomatology; National Clinical Research Center for Oral Diseases; Shanghai Key Laboratory of Stomatology, Shanghai, PR China.
[c]Graduate student, Department of Prosthodontics, Shanghai Ninth People's Hospital, Shanghai Jiao Tong University School of Medicine; College of Stomatology, Shanghai Jiao Tong University; National Center for Stomatology; National Clinical Research Center for Oral Diseases; Shanghai Key Laboratory of Stomatology, Shanghai, PR China.
[d]Associate Professor, Department of Research Management, Yangpu Hospital, School of Medicine, Tongji University, Shanghai, Shanghai, PR China.
[e]Full Professor, Department of Stomatology, Yangpu Hospital, School of Medicine, Tongji University, Shanghai, PR China.
[f]Dental Prosthetic Technician, Prosthodontic Technician Center, Shanghai Ninth People's Hospital, Shanghai Jiao Tong University School of Medicine; College of Stomatology, Shanghai Jiao Tong University; National Center for Stomatology; National Clinical Research Center for Oral Diseases; Shanghai Key Laboratory of Stomatology, Shanghai, PR China.
[g]Associate Professor, Department of Prosthodontics, Shanghai Ninth People's Hospital, Shanghai Jiao Tong University School of Medicine; College of Stomatology, Shanghai Jiao Tong University; National Center for Stomatology; National Clinical Research Center for Oral Diseases; Shanghai Key Laboratory of Stomatology, Shanghai Research Institute of Stomatology, Shanghai, PR China.
[1]Y. L. and Y. H. contributed equally to this article.

Clinical Implications

Connectors designed with a rectangular 5×4-mm cross-section are recommended to disperse occlusal force and improve the resistance of the restoration. The contact-point retainer meets the clinical requirements of cantilever RBFPDs to replace maxillary lateral incisors, whether placed on the labial or palatal side.

Congenitally missing permanent maxillary lateral incisors are common, affecting about 0.8% to 2% of the population.[1] Missing lateral incisors may also arise from trauma,[2] periodontal disease,[3] or endodontic failure.[4] The absence not only undermines dental arch integrity but also presents significant esthetic, emotional, and social hurdles for patients.[3,5]

Options for replacing missing maxillary lateral incisors include implant-supported single crowns,[6,7] orthodontic space closure,[7] crown-retained fixed partial dentures (FPDs), and resin-bonded fixed partial dentures (RBFPDs). Dental implants, recognized for their esthetic appeal and high long-term survival rates of up to 96% in the anterior maxilla,[8] need sufficient space and proper tissue conditions.[7] Furthermore, young patients with tooth loss may not be eligible for implants.[9] Orthodontic closure, which involves closing the space and reshaping adjacent teeth, is often the preferred option but may be contraindicated for patients with concave facial profiles because of the risk of exacerbating Class III skeletal patterns.[7] Although complete coverage FPDs have been reported to be an effective option, significant preparation of undamaged abutment teeth is needed, potentially compromising their long-term pulpal health.[10] Conversely, RBFDPs offer a conservative interim or definitive option, minimizing esthetic and pulpal health risks and serving as a suitable option when an implant-supported crown is not feasible.

RBFDPs include retainers, connectors, and pontics. A significant advancement in their design was the introduction of a cantilever rather than the 2-abutment designs by Kern and Gläser in 1997[11] which prevented differential abutment mobility and the associated risks of debonding and secondary caries.[12] The cantilever design is particularly advantageous for replacing missing maxillary lateral incisors.[13] Among RBFPD materials, zirconia offers robust durability but may be prone to debonding.[14] Lithium disilicate provides superior esthetics and bonding,[15] although its susceptibility to fracture requires an optimal design.[16]

The efficacy of lithium disilicate cantilever RBFPDs has been reported to be influenced by crucial design elements, including retainer positioning,[17] whether on the labial or palatal side,[4] the bonded area,[18] the connector volume[19] and morphology,[20] and the retainer type.[21] Traditionally, veneer retainers have been the preferred choice, with research exploring their positioning and the effects of the connector shape in conventional RBFPD designs.[12,13,22] For missing lateral incisors, canine retainers have been widely advocated[23,24] owing to the superior stress distribution and strong periodontal support of canines. Placing retainers labially allows the reshaping of the abutment teeth and avoids occlusal interference in patients with vertical overlap.[25] Conversely, lingual retainer placement preserves the esthetics of the abutment tooth; furthermore, supplementary retention grooves may be incorporated.[26] The connector shape also holds significance as rectangular connectors ensure an even stress distribution, whereas trapezoidal connectors offer a less visible alternative.[19]

Gresnigt et al[27] recently introduced an innovative contact-point RBFPD design to minimize the bonded interface by strategically ending the cantilever retainer at the interproximal and palatal margins. Compared with veneer-retainer RBFPDs, the contact-point RBFPD prosthesis offers advantages, including reduced tooth preparation with a minimally invasive approach.[28] The authors also reported a 100% five-year success rate with the contact-point design.[27] Additionally, the perimeter of the retainer is minimized, lowering the risk of caries.[4,27,29] Nevertheless, scientific experiments to validate the force distribution across each tooth in a contact-point RBFPD are lacking. It remains uncertain whether the restorative outcomes align with those previously reported when the clinically required adhesion area is not adequately met[18] and whether comprehensive in vitro or finite element analysis (FEA) comparisons across various design factors are needed.[19,29,30] RBFPD evaluations have been drawn from clinical studies[19,21,23,30,31] with minimal to no assessment of resin-bonded design parameters, especially the connector shape and retainer design.[13,19]

This study aimed to augment the clinical understanding of the RBFPD design of lithium disilicate cantilevers through FEA. Owing to the complexity of the design factors, the stress distributions across different combinations of retainer placements, connector shapes, and retainer types were evaluated. The labial veneer RBFPD (LV-RBFPD), palatal veneer RBFPD (PV-RBFPD), labial contact-point RBFPD (LC-RBFPD), and palatal contact-point RBFPD (PC-RBFPD) designs were examined in conjunction with rectangular and trapezoidal connectors. The null hypothesis was that no difference in stress distribution would be found among the various designs under identical loading conditions.

MATERIAL AND METHODS

The study was approved by the local ethics committee (certificate of presentation for ethical consideration LL-

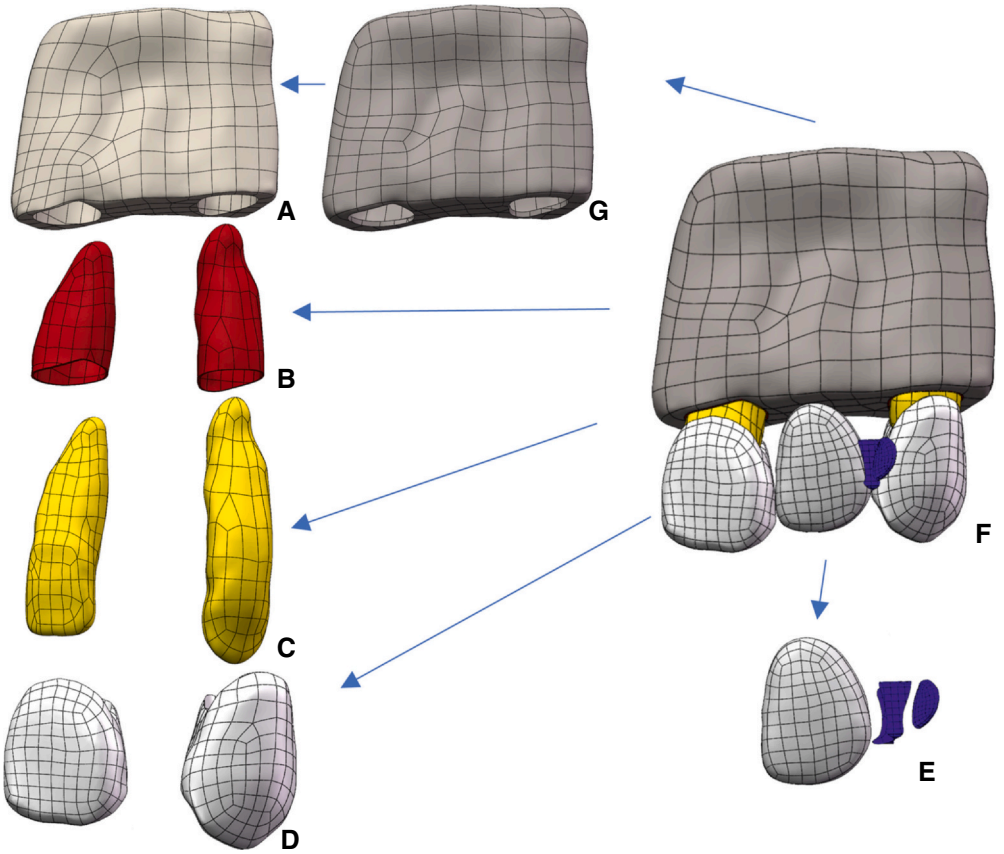

Figure 1. Schematic of 3-dimesional models. A, Cancellous bone. B, Periodontal ligaments. C, Dentin. D, Enamel. E, Prosthesis. F, Unstratified model. G, Cortical bone.

2024-QSW-023). Signed informed consent following the Helsinki guidelines was obtained from the volunteers. Using cone beam computed tomography (CBCT) data from a healthy volunteer, a unilateral maxillary anterior dentition model (Fig. 1) was created to simulate the absence of the left maxillary lateral incisor. The CBCT scans had been conducted using a machine (HiRes3D-Plus; LARGEV) with a tube voltage of 120 kV, a tube current of 5 mA, an irradiation time of 4.05 seconds, a slice thickness of 250 μm, and a table speed of 1 mm/second. The acquired Digital Imaging and Communications in Medicine (DICOM) data were processed in a software program (Mimics Medical 21.0; Materialize NV) where cortical and cancellous bone, dentin, and enamel were reconstructed and converted into standard tessellation language (STL) files.

In a mesh editing program (Geomagic Wrap 2021; 3D Systems Inc), adjustments were made to the dentition components, and prostheses were designed accordingly. A 0.2-mm-thick periodontal ligament (PDL) layer was created. Two connector types were modeled: one rectangular (5×4 mm) and the other trapezoidal (5×4×1 mm) in shape (Fig. 2). Four retainer types were used for the canine: LV-RBFPD, PV-RBFPD, LC-RBFPD, and PC-RBFPD, each approximately 0.3-mm thick (Fig. 3). The LV-RBFPD and the PV-RBFPD required 0.3-mm tooth preparation to accommodate the thickness of the RBFPD,[21] with labial veneers covering the entire labial surface and lingual veneers, including the nonocclusal guiding areas of the lingual surface. In contrast, contact-point retainers needed no preparation and terminated at the junction of the labial (or palatal) and proximal surfaces. The pontic had a ridge-lap shape.[27]

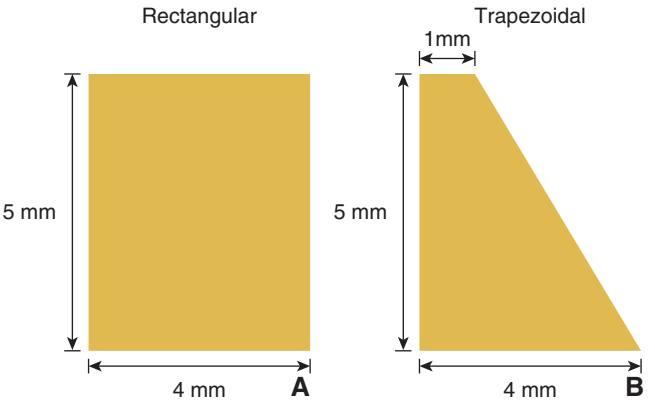

Figure 2. A, Rectangular cross-sectional shape. B, Trapezoidal cross-sectional shape.

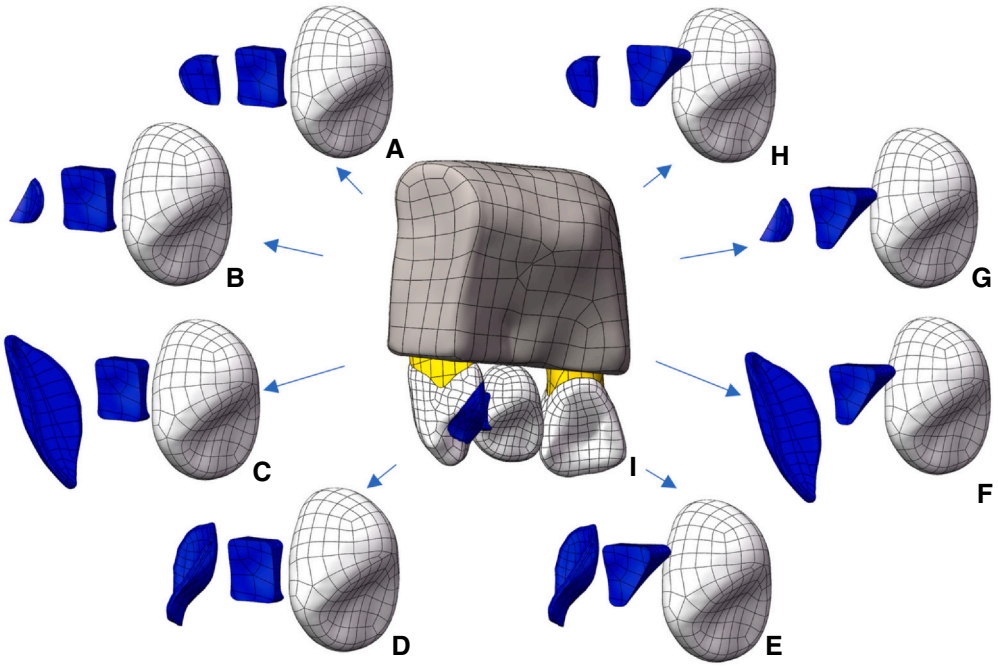

Figure 3. Configurations of RBFPDs. A-D, Rectangular connectors. A, Labial contact-point RBFPD (R-LC-RBFPD). B, Palatal contact-point RBFPD (R-PC-RBFPD). C, Labial veneer RBFPD (R-LV-RBFPD). D, Palatal veneer RBFPD (R-PV-RBFPD). E-H, Trapezoidal connectors. E, Palatal veneer RBFPD (T-PV-RBFPD). F, Labial veneer RBFPD (T-LV-RBFPD). G, Palatal contact-point RBFPD (T-PC-RBFPD). H, Labial contact-point RBFPD (T-LC-RBFPD). I, Alveolar and dental structures with RBFPD. RBFPD, resin-bonded fixed partial denture.

Table 1. Element size and material properties

Material	Element Size (mm)	Modulus of Elasticity (MPa)	Poisson Ratio (υ)	Reference
Enamel	0.4	84 100	0.31	[29]
Dentine	0.4	18 600	0.31	[29]
Periodontal ligament	0.4	0.23	0.49	[30]
Cortical bone	0.8	13 700	0.3	[32]
Cancellous bone	0.8	1370	0.3	[33]
Lithium disilicate	0.2	95 000	0.22	[34]

The models were exported to an FEA program (SolidWorks 2023; Dassault Systems) in the standard for the exchange of product data (STEP) format, and Boolean operations were conducted in the PART file (the storage format of the SolidWorks software program). These assembled computer-aided design (CAD) models were then imported into a simulation software program (Ansys 2024 R1; ANSYS Inc) for structural static analysis. All the materials, other than the periodontal ligaments, were assumed to be homogeneous, isotropic, and linearly elastic; the properties of the periodontal ligaments were considered heterogeneous and viscoelastic stress-strain behavior (Table 1). The mechanical properties of a commercially available ceramic (IPS e.max CAD; Ivoclar AG) were used to represent lithium disilicate.[35] Tetrahedral elements of appropriate sizes were automatically meshed for the models (Table 1). All contact surfaces within the models were considered fully bonded, and the cranial surface of the maxillary cortical bone was restricted in all degrees of freedom. Loading conditions included regional loading[19,36–38] and point loading[23] to simulate different stress scenarios. Based on previous studies,[39–42] a force of 100 N was selected for application to the restoration, regardless of whether it was a regional load or a point load.[32] Regional loading applied a 100-N force at a 45-degree angle to the long axis of the pontic's incisal third, mimicking extreme conditions that could lead to debonding or fracture. Point loading involves applying 100-N forces perpendicular to the surfaces of the teeth or pontic,[18] with the interproximal contact area varying according to different mandibular occlusion positions, including the maximal intercuspal position, protrusive, and lateral positions, simulating physiological mastication conditions[41] (Fig. 4). The maximum von Mises stress, the maximum principal stress, and the minimum principal stress for each scenario were then computed.

RESULTS

To integrate the connector, base, and fixed partial denture into a unified assembly, Boolean operations were used,[30] and the volumes of the rectangular and trapezoidal connectors were calculated as 10.0 mm^3 and 9.6 mm^3, respectively, via the simulation software

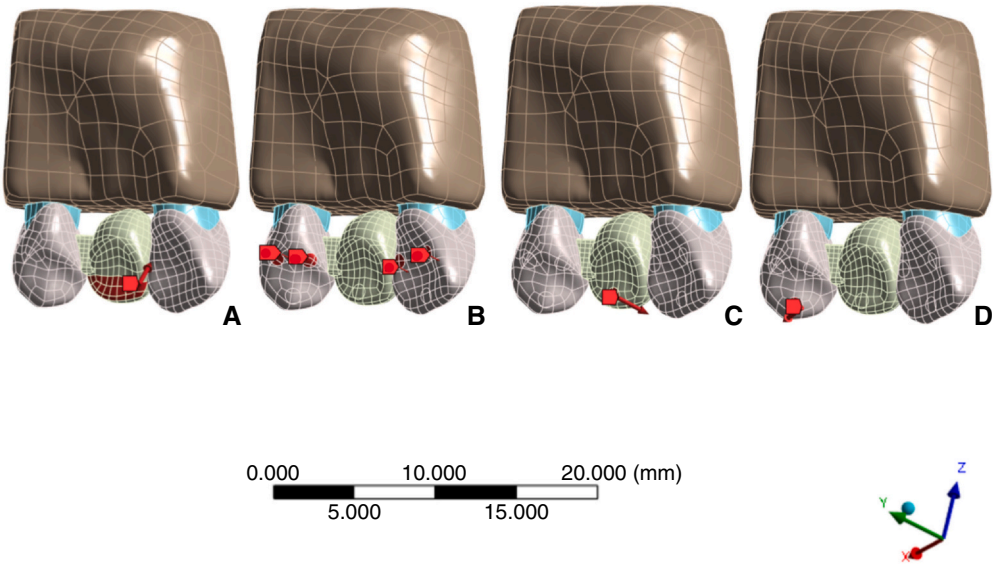

Figure 4. Loading conditions. A, Regional loading: 100-N force applied at 45-degree angle to pontic's incisal third. B-D, Point loading: 100-N force applied perpendicularly at each 0.6-mm point contact in maximal intercuspal position (B), protrusive position (C), and lateral position (D).

Table 2. Connector volume and retainer volume

Connector Shape	Retainer Type	Dimensions (mm)	Cross-sectional area (mm^2)	Connector Volume (mm^3)	Bonding surface area (mm^2)
Rectangular	LC	Length:5 Width:4	20	10.048	16.93
	LV				66.78
	PC				16.78
	PV				39.45
Trapezoidal	LC	Height:5 Baseline:4 Topline:1	12.5	9.6194	14.99
	LV				65.08
	PC				16.02
	PV				38.78

LC, labial contact point; LV, labial veneer; PC, palatal contact point; PV, palatal veneer.

program (Ansys 2024 R1; ANSYS Inc). Additionally, the FEA software program (SolidWorks 2023; Dassault Systems) was used to determine the bonding surface areas between each RBFPD and the abutment (Table 2).

Figures 5 to 7 show qualitative maps of the von Mises stresses on the external surfaces of the RBFPDs under the 4 loading conditions, and the maximum stress peak for each structure was recorded using an autoprobe. In general, the maximal values of the equivalent stresses appeared at the connectors under most loading conditions. However, the shape of the connector's cross-section influenced the magnitude of the stress peaks. Table 3 summarizes the estimated maximum equivalent stresses. The rectangular connector groups presented lower stress concentrations than the trapezoidal connector groups, regardless of the design of the retainer. Under point contact loading at the protrusion position, in the rectangular connector groups, the maximum von Mises stresses in the LC-RBFPD and PC-RBFPD groups were lower than those in the LV-RBFPD and PV-RBFPD groups. Despite these slight differences, the stress values ranged from 46.7 MPa to 450.0 MPa across all the models with rectangular connectors.

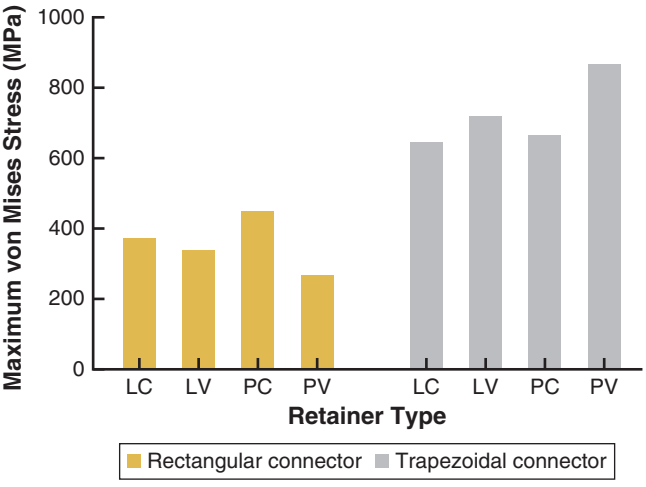

Figure 5. Comparison of maximum von Mises stresses of two types of retainers.

Fig. 8 and Table 4 primarily illustrate the maximum principal stress distribution across each group. Concerning the distribution of the maximum principal stress,

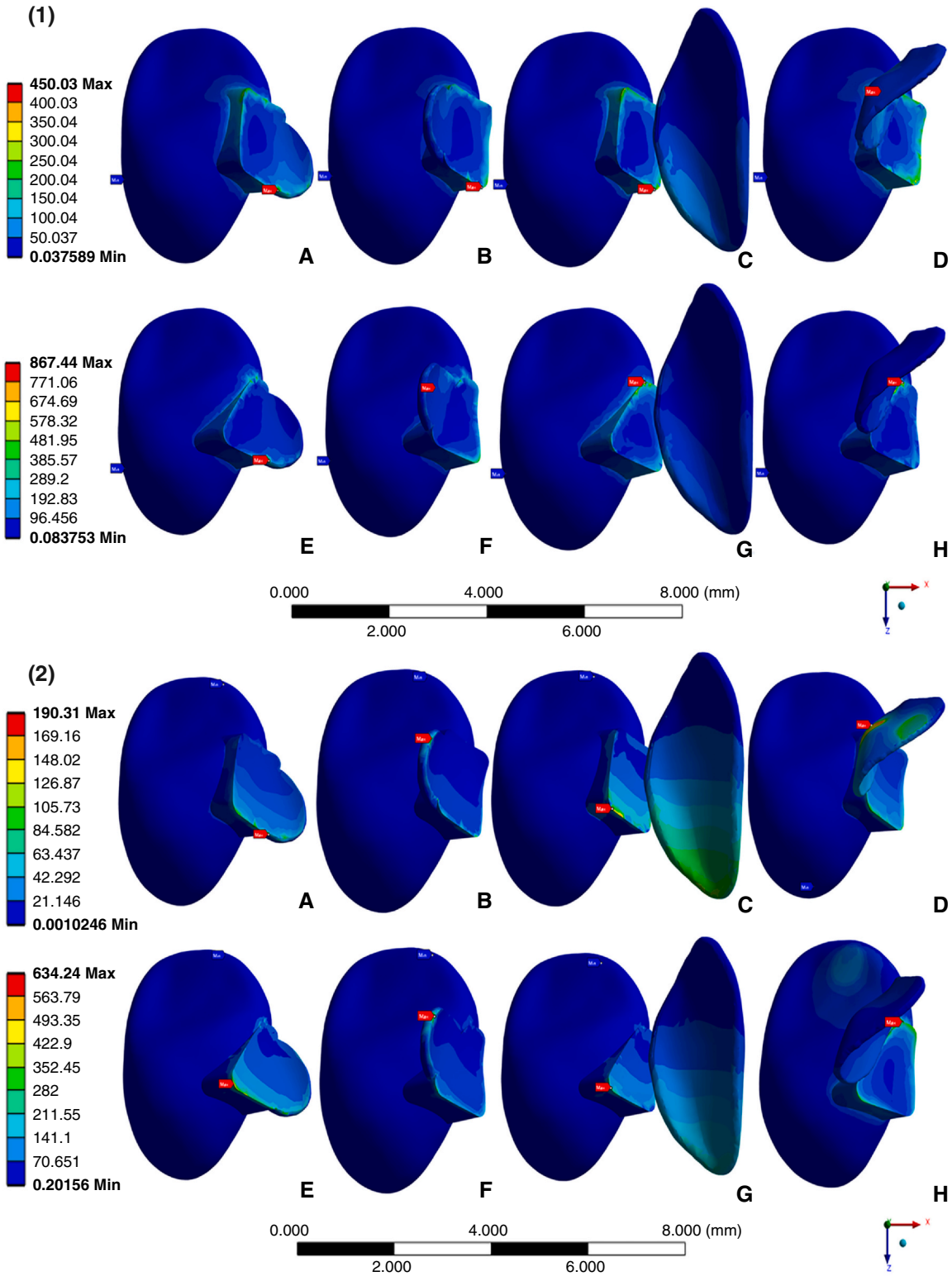

Figure 6. (1) Maximum von Mises stress distribution under regional loading. (2) Maximum von Mises stress distribution under point contact loading at maximal intercuspal position. (3) Maximum von Mises stress distribution under point contact loading in protrusive position. (4) Maximum von Mises stress distribution under point contact loading in lateral position. A-D, Rectangular connections: A, Labial contact-point RBFPD (R-LC-RBFPD). B, Palatal contact-point RBFPD (R-PC-RBFPD). C, Labial veneer RBFPD (R-LV-RBFPD). D, Palatal veneer RBFPD (R-PV-RBFPD). E-H, Trapezoidal connectors. E, Labial contact-point RBFPD (T-LC-RBFPD). F, Palatal contact-point RBFPD (T-PC-RBFPD). G, Labial veneer RBFPD (T-LV-RBFPD). H, Palatal veneer RBFPD (T-PV-RBFPD). RBFPD, resin-bonded fixed partial denture.

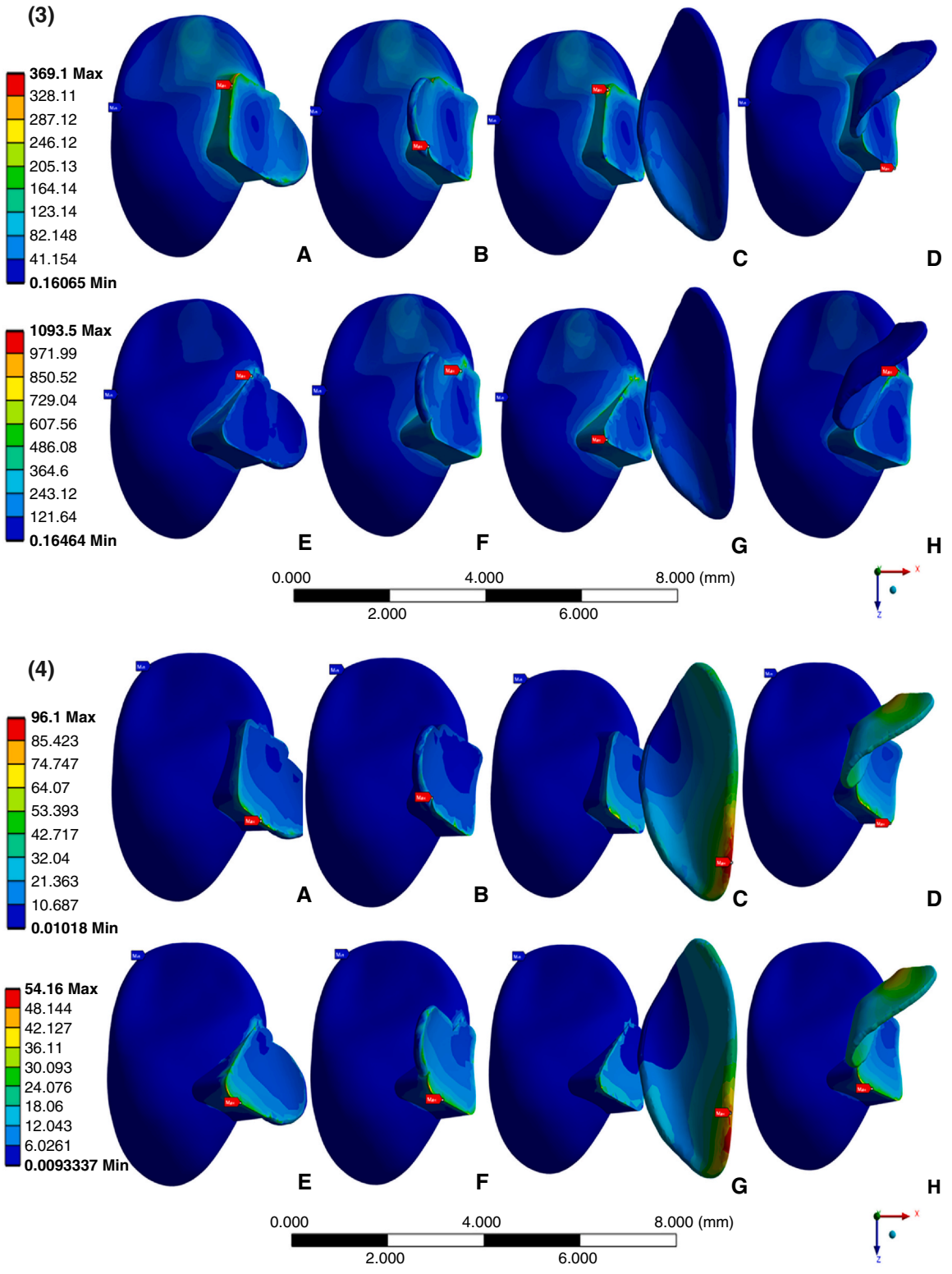

Figure 6. (*continued*)

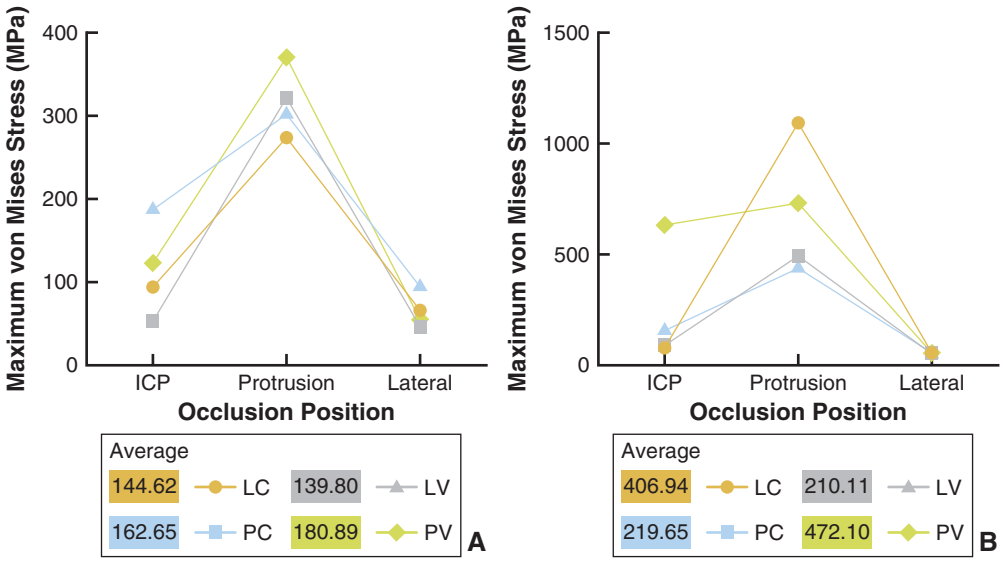

Figure 7. Stress distribution in each group under three occlusion positions. A, Rectangular connector group. B, Trapezoidal connector group.

Table 3. Maximum von Mises stress in each group

Connector Type	Maximum von Mises Stress (MPa)	Labial				Palatal			
		45-degree	Maximal Intercuspal	Protrusion	Lateral	45-degree	Maximal Intercuspal	Protrusion	Lateral
Rectangular Connector	Contact-point Veneer	376.520 339.470	94.100 52.023	273.400 320.930	66.082 46.674	450.030 268.500	190.310 122.350	301.930 369.100	96.100 51.578
Trapezoidal Connector	Contact-point Veneer	821.730 720.600	75.512 85.577	1093.500 493.700	51.166 48.526	663.530 867.740	168.870 634.240	435.690 731.790	54.160 50.263

peak values for each type of RBFPD were observed at the junction between the connector and its interface with the retainer. Under the 45-degree loading conditions, the stress concentration in the rectangular connector groups was lower than that in the trapezoidal connector groups during the lateral orientation; this may be attributed to direct loading on the abutment teeth in this position. In the contact-point loading conditions of the protrusive positions, in the rectangular connector groups, the maximum principal stresses within the LC-RBFPD and PC-RBFPD groups were lower than those in the LV-RBFPD and PV-RBFPD groups, with PV-RBFPD exhibiting a peak value of 490.2 MPa—exceeding the bend strength threshold of lithium disilicate (470 MPa)—suggesting a potential risk for structural compromise under extreme conditions.[43] Despite these minor variations, the stress values across all the models equipped with rectangular connectors ranged from 38.7 MPa to 490.2 MPa.

Fig. 9 and Table 5 primarily illustrate the distribution of the minimum principal stress within each group of prostheses. Minimum principal stress is essential for evaluating whether the thin-walled structure of a prosthesis may experience local buckling because of excessive compressive forces.[44] The stress values across all the models featuring rectangular connectors ranged from 1.0 MPa to 85.5 MPa, indicating that the 4 sets of restorations with rectangular connectors exhibited less internal deformation under loading than those in the trapezoidal group.

DISCUSSION

The study results revealed differences in stress distribution among the different designs; therefore, the null hypothesis that no difference would be found in stress distribution among the various designs under identical loading conditions was rejected. In scenarios where the volume of the connection body is comparable, an increase in the cross-sectional area of the connection body correlates with reduced stress. Furthermore, within the rectangular labial groups, the stress values for both the contact-point retainers and veneer retainers do not exceed the bend strength threshold of the lithium disilicate material. Additionally, the design of contact-point retainers offers the advantage of eliminating the need for tooth preparation.

While the von Mises stress criterion has been generally considered less relevant for brittle materials such

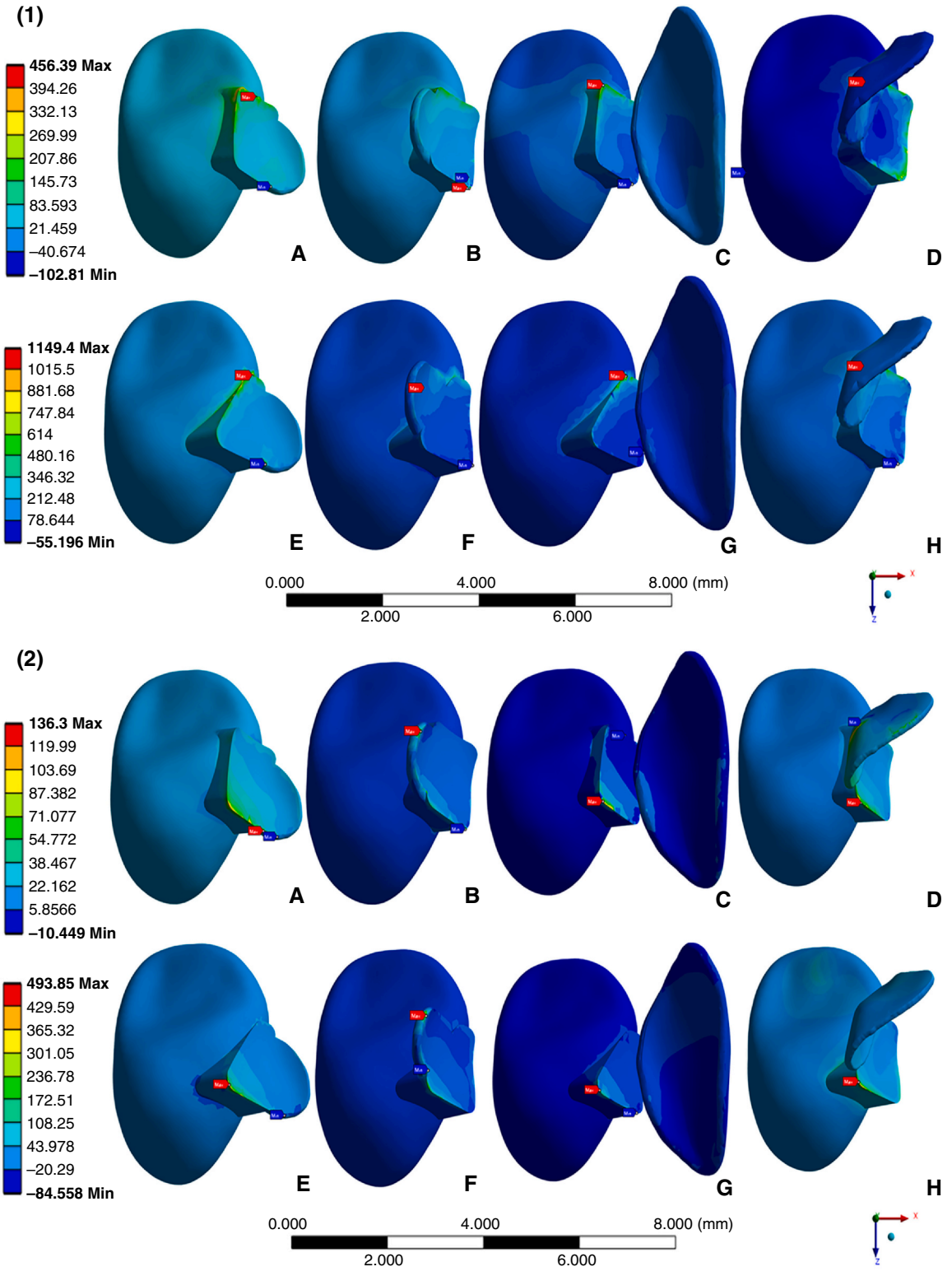

Figure 8. (1) Maximum principal stress distribution under regional loading. (2) Maximum principal stress distribution under point contact loading at maximal intercuspal position. (3) Maximum principal stress distribution under point contact loading at protrusive position. (4) Maximum principal stress distribution under point contact loading in lateral position. A-D, Rectangular Connectors. A, R-LC-RBFPD. B, R-PC-RBFPD. C, R-LV-RBFPD. D, R-PV-RBFPD. E-H, Trapezoidal connectors. E, T-LC-RBFPD. F, T-PC-RBFPD. G, T-LV-RBFPD. H, T-PV-RBFPD. RBFPD, resin-bonded fixed partial denture.

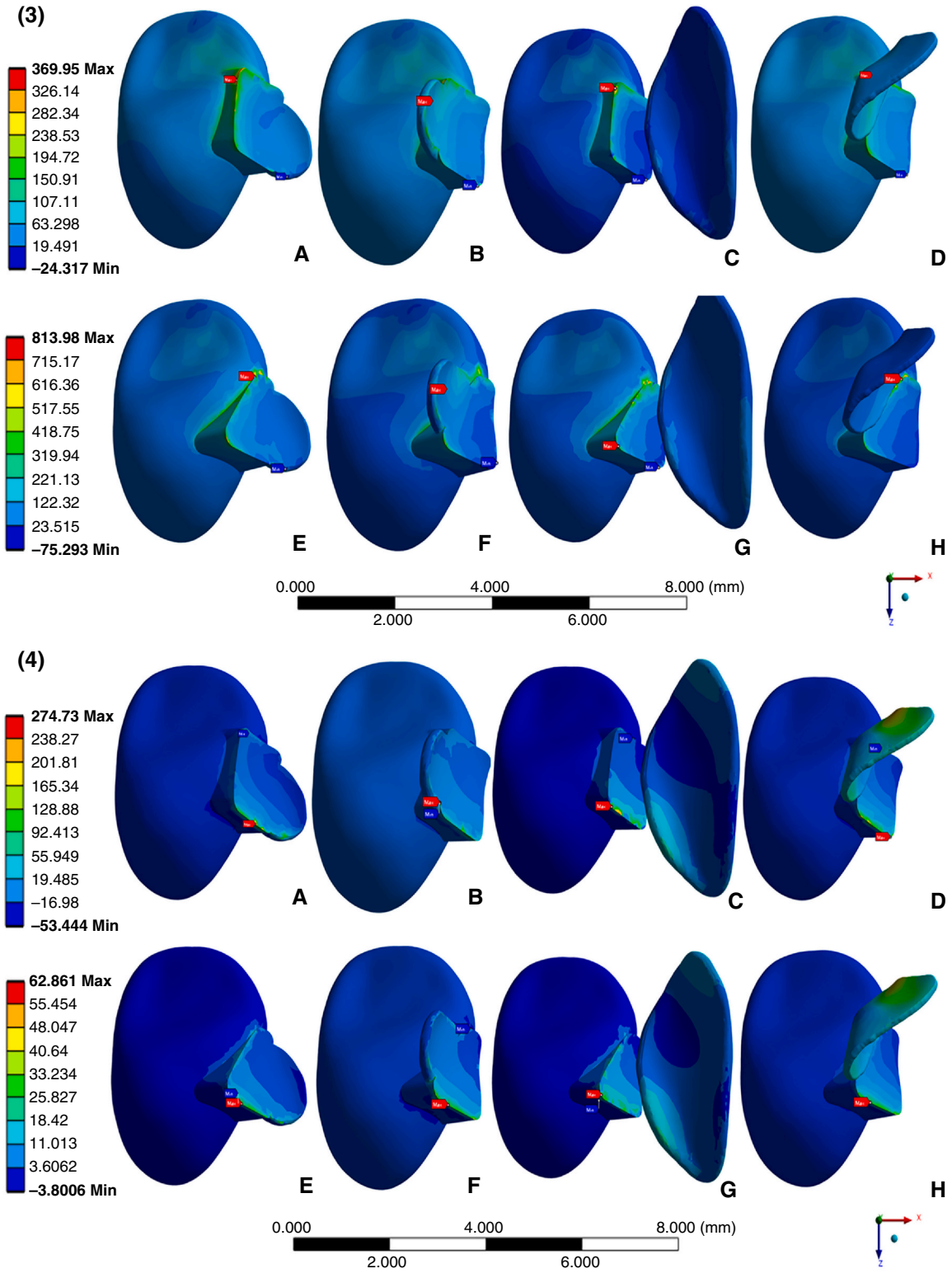

Figure 8. (*continued*)

Table 4. Maximum principal stress in each group

Connector Type	Maximum Principal Stress (MPa)	Labial				Palatal			
		45-degree	Maximal Intercuspal	Protrusion	Lateral	45-degree	Maximal Intercuspal	Protrusion	Lateral
Rectangular Connector	Contact-point	348.230	54.114	307.540	59.426	456.390	136.300	356.040	101.750
	Veneer	389.880	47.509	369.950	38.711	386.970	86.552	366.840	52.679
Trapezoidal Connector	Contact-point	512.770	86.340	507.740	58.522	687.590	138.110	462.140	62.861
	Veneer	948.150	100.070	552.090	37.669	1149.400	493.850	813.980	59.081

as teeth and ceramics,[23] it was included in this study for comparison with existing studies on RBFPDs.[19,30] After 4 types of loading were applied, rectangular connectors reduced the stress distribution under all conditions. In contrast, most trapezoidal groups exhibited clinically unacceptable stress distributions, particularly under contact loading in the protrusive position. Moreover, contact-point RBFPDs paired with rectangular connectors generally presented lower maximum von Mises values than paired veneer RBFPDs under contact loading, simulating physiological conditions, consistent with the in vitro findings of Gresnigt et al.[4] The stress distribution in rectangular connector RBFPDs outperforms that in trapezoidal connectors, effectively dispersing stress within the fracture threshold of lithium disilicate, consistent with the findings of Osman et al,[19] who indicated that the maximum von Mises stress distribution on the connector decreased as the volume of the connector increased.

By evaluating the tensile stresses, the maximum principal stress helped identify the region most susceptible to microcracks and fractures. In this study, the maximum principal stress values obtained under 100-N regional loading ranged from 37.7 MPa to 1200 MPa, consistent with a previous study.[19,23,30] However, the maximum principal stress values in some groups under point loading at the protrusive position exceeded the biaxial strength of the commercially available ceramic (IPS e.max CAD; Ivoclar AG) (470 ±60 MPa) according to the manufacturer's specifications. This discrepancy could be attributed to the loading conditions, where the force was directly applied to the pontic. Furthermore, the selection of a 100-N load was motivated primarily by previous studies,[30,39–42] where loading forces ranging from 10 N to 200 N were used. Abe et al[39] calculated the occlusal force of individual teeth via specialized analytical equipment and a software program. The occlusal force on the maxillary lateral incisor during mandibular functional movements did not exceed 100 N, consistent with Wang et al.[40] In actual clinical scenarios, the pontic should only experience light or no contact and should not primarily bear the occlusal force.

The minimum principal stress provides a complementary view of the internal stress state within the material by distinguishing regions where stress is unevenly distributed; these areas can become the starting points for stress concentration, leading to the formation and propagation of cracks. In this study, the minimum principal stress concentration locations were predominantly identified in the connection area, with only a few instances observed at the edge of the retainer during protrusion and in the lateral position.

This study reveals that when the volumes of rectangular and trapezoidal connectors were comparable, the cross-sectional area of the rectangular connector exceeded that of its trapezoidal counterpart. Nevertheless, across all 4 loading scenarios, the stress distribution in the design of the rectangular connector remained lower than that observed in the trapezoidal connector. Increasing the cross-sectional area of the connector can effectively reduce stress, as it results in a greater moment of inertia, thereby improving the resistance of the connector to bending deformation and facilitating a more uniform distribution of external forces; this mitigates local stress concentrations and reduces the risk of brittle fractures.

The CBCT data of an Asian female patient were selected for this study, which restricted the mesial surface area of the canines in the models; however, if the small teeth can accommodate a sufficient volume of the connecting element, then the data derived should be applicable to larger teeth. Patients with larger tooth dimensions may have a wider array of design choices in clinical practice, potentially including RBFPDs with trapezoidal connectors. Gresnigt et al[27] used the lost-wax casting technique to fabricate contact-point RBFPDs, which frequently have limitations in the precise shape design of connectors. Computer-aided design and computer-aided manufacturing (CAD-CAM) technology facilitates more accurate design and precise milling. Additionally, the technical intricacy of these restorations mandates the use of a digitally designed 3-dimensional (3D) printed guide to ensure proper placement.[3]

Limitations of the present study included that only static loading was used to validate the optimized designs. In contrast, clinically, the majority of dental restorations fail under cyclic loading with a lower force. In addition, the FEA could not simulate all the clinical conditions exactly owing to the simplifications and approximations of the models. Future research should validate these findings through in vitro and clinical

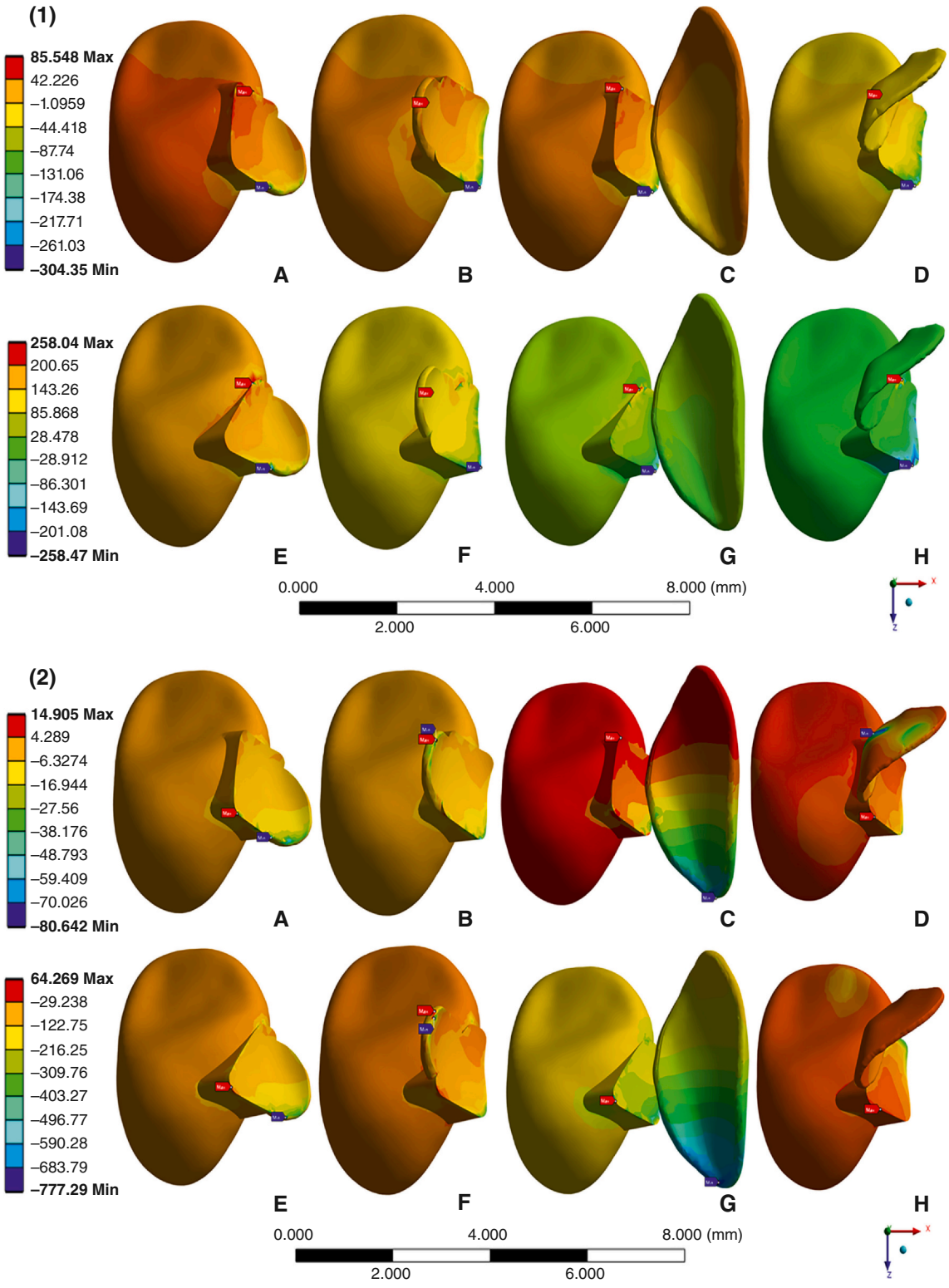

Figure 9. (1) Minimum principal stress distribution under regional loading. (2) Minimum principal stress distribution under point contact loading at maximal intercuspal position. (3) Minimum principal stress distribution under point contact loading in protrusive position. (4) Minimum principal stress distribution under point contact loading in lateral position. A-D, Rectangular connectors. A, R-LC-RBFPD. B, R-PC-RBFPD. C, R-LV-RBFPD. D, R-PV-RBFPD. E-H, Trapezoidal connectors. E, T-LC-RBFPD. F, T-PC-RBFPD. G, T-LV-RBFPD. H, T-PV-RBFPD. RBFPD, resin-bonded fixed partial denture.

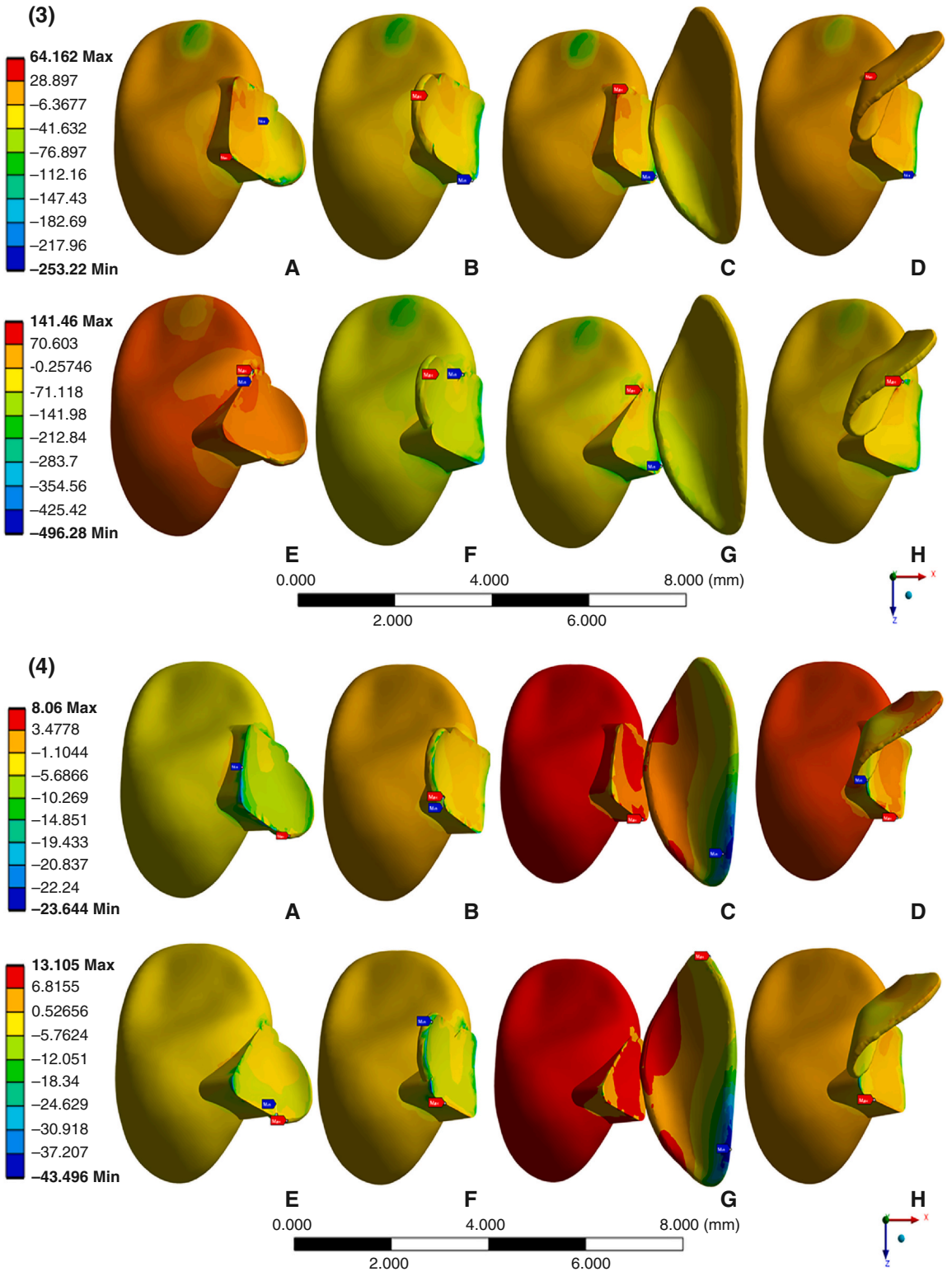

Figure 9. (*continued*)

Table 5. Minimum principal stress in each group

Connector Type	Minimum Principal Stress (MPa)	Labial				Palatal			
		45-degree	Maximal Intercuspal	Protrusion	Lateral	45-degree	Maximal Intercuspal	Protrusion	Lateral
Rectangular	Contact-point	49.117	11.435	38.280	8.060	61.578	14.905	64.162	7.354
Connector	Veneer	54.599	1.036	41.654	2.162	85.548	9.723	62.045	2.362
Trapezoidal	Contact-point	130.800	10.066	119.130	13.105	129.340	9.535	134.310	7.400
Connector	Veneer	212.430	11.813	107.950	2.023	258.040	64.249	141.460	7.692

studies to enhance the understanding of the clinical implications of these designs.

CONCLUSIONS

Based on the findings of this FEA study, the following conclusions were drawn:

1. The rectangular cross-sectional design of the connector in all the groups could help disperse occlusal force and improve the resistance of the restoration.
2. Both the veneer and contact-point retainer in the rectangular group were clinically acceptable and were able to resist fracture.

REFERENCES

1. Alqahtani H. Association between sella turcica bridging and congenitally missing maxillary lateral incisors. *J Dent Sci*. 2020;15:59–64.
2. Petersen FN, Jensen SS, Dahl M. Implant treatment after traumatic tooth loss: A systematic review. *Dent Traumatol*. 2022;38:105–116.
3. Kim T, Lee S, Kim GB, et al. Accuracy of a simplified 3D-printed implant surgical guide. *J Prosthet Dent*. 2020;124:195–201.
4. Gresnigt MMM, Tirlet G, Bosnjak M, Made SVD, Attal JP. Fracture strength of lithium disilicate cantilever resin bonded fixed dental prosthesis. *J Mech Behav Biomed Mater*. 2020;103:103–115.
5. Imam AY. Impact of tooth loss position on oral health-related quality of life in adults treated in the community. *J Pharm Bioallied Sci*. 2021;13:969–974.
6. Priest G. The treatment dilemma of missing maxillary lateral incisors-Part II: Implant restoration. *J Esthet Restor Dent*. 2019;31:319–326.
7. Jamilian A, Perillo L, Rosa M. Missing upper incisors: A retrospective study of orthodontic space closure versus implant. *Prog Orthod*. 2015;16:2.
8. Winitsky N, Olgart K, Jemt T, Smedberg JI. A retro-prospective long-term follow-up of Brånemark single implants in the anterior maxilla in young adults. Part 1: Clinical and radiographic parameters. *Clin Implant Dent Relat Res*. 2018;20:937–944.
9. Knobloch LA, Larsen P, Mcglumphy E, et al. Fogarty prospective cohort study to evaluate narrow diameter implants for restoration of a missing lateral incisor in patients with a cleft palate: One-year results. *J Prosthet Dent*. 2022;128:1265–1274.
10. Fathi A, Rismanchian M, Khodadadi R, Dezaki SN. Does the crown-implant ratio affect the survival and complications of implant-supported prostheses? A systematic review. *J Prosthet Dent*. 2024;131:819–825.
11. Kern M, Gläser R. Cantilevered all-ceramic, resin-bonded fixed partial dentures: A new treatment modality. *J Esthet Dent*. 1997;9:255–264.
12. Mourshed B, Samran A, Alfagih A, Samran A, Abdulrab S, Kern M. Anterior cantilever resin-bonded fixed dental prostheses: A review of the literature. *J Prosthodont*. 2018;27:266–275.
13. Mine A, Fujisawa M, Miura S, et al. Critical review about two myths in fixed dental prostheses: Full-Coverage vs. resin-bonded, non-cantilever vs. cantilever. *Jpn Dent Sci Rev*. 2021;57:33–38.
14. Klink A, Hüttjg F. Zirconia-based anterior resin-bonded single-retainer cantilever fixed dental prostheses: A 15- to 61-month follow-up. *Int J Prosthodont*. 2016;29:284–286.
15. Zarone F, Dimauro MI, Ausiello P, Ruggiero G, Sorrentino R. Current status on lithium disilicate and zirconia: A narrative review. *BMC Oral Health*. 2019;19:134.
16. Di Fiore A, Stellini E, Savio G, Rosso S, Graiff L, Granata S. Assessment of the different types of failure on anterior cantilever resin-bonded fixed dental prostheses fabricated with three different materials: An in vitro study. *Appl Sci (Basel)*. 2020;10:12.
17. Kern M, Gläser R. Single-retainer all-ceramic resin-bonded fixed dental prostheses: Long-term outcomes in the esthetic zone. *J Esthet Restor Dent*. 2023;35:64–73.
18. Kern M. Resin-bonded fixed dental prostheses. London: Quintessence,; 2018:141.
19. Osman MLM, Lim TW, Chang HC, ARAb Ghani, Tsoi JKH, SMAb Ghani. Structural integrity of anterior ceramic resin-bonded fixed partial denture: A finite element analysis study. *J Funct Biomater*. 2023;14:108.
20. Wei YR, Wang XD, Zhang Q, et al. Clinical performance of anterior resin-bonded fixed dental prostheses with different framework designs: A systematic review and meta-analysis. *J Dent*. 2016;47:1–7.
21. Naguib A, Fahmy N, Hamdy A, Wahsh M. Fracture resistance of different designs of a resin-bonded fixed dental prosthesis: An in vitro study. *Int J Prosthodont*. 2021;34:348–356.
22. Thoma DS, Sailer I, Ioannidis A, Zwahlen M, Makarov N, Pjetursson BE. A systematic review of the survival and complication rates of resin-bonded fixed dental prostheses after a mean observation period of at least 5 years. *Clin Oral Implants Res*. 2017;28:1421–1432.
23. Kihara T, Shigeta Y, Ikawa T, Sasaki K, Shigemoto S, Ogawa T. Designing anterior cantilever resin-bonded fixed dental prostheses based on finite element analysis. *J Prosthodont Res*. 2023;67:418–423.
24. Botelho MG, Ma X, Cheung GJ, Law RKS, Tai MTC, Lam WYH. Long-term clinical evaluation of 211 two-unit cantilevered resin-bonded fixed partial dentures. *J Dent*. 2014;42:778–784.
25. Türkaslan S, Mutluay MM, Vallittu PK, Arola D, Tezvergil-Mutluay A. Fatigue resistance of metal-free cantilever bridges supported by labial laminate veneers. *J Mech Behav Biomed Mater*. 2020;103:596.
26. Habibzadeh S, Khamisi F, Mosaddad SA, Fernandes GV de O, Heboyan A. Full-ceramic resin-bonded fixed dental prostheses: A systematic review. *J Appl Biomater Funct Mater*. 2024;22:228.
27. Gresnigt MMM, Jonker JA, Van Der Made SAM. The cantilever contact-point resin bonded bridge; adhesion 2.0. *J Esthet Restor Dent*. 2024;36.
28. Diab M, Karkoutly M, Kanout S, Nassar JA. Effect of a novel mesh design and the sandblasting technique on the bond strength of computer-designed and three-dimension laser printed resin bonded bridges: an in vitro study. *Sci Rep*. 2024;14:8412.
29. Trindade FZ, Valandro LF, De Jager N, Bottino MA, Kleverlaan CJ. Elastic properties of lithium disilicate versus feldspathic inlays: Effect on the bonding by 3D finite element analysis. *J Prosthodont*. 2018;27:741–747.
30. Sorrentino R, Apicella D, Riccio C, et al. Nonlinear visco-elastic finite element analysis of different porcelain veneers configuration. *J Biomed Mater Res B Appl Biomater*. 2009;91:727–736.
31. Pattaratiwanont R, Piemjai M, Garcia-godoy F. Survival of posterior fixed partial dentures with minimal tooth reduction and improved esthetics: An in vitro study. *J Prosthet Dent*. 2022;127:585–592.
32. Uraba A, Nemoto R, Nozaki K, Inagaki T, Omori S, Miura H. Biomechanical behavior of adhesive cement layer and periodontal tissues on the restored teeth with zirconia RBFDPs using three-kinds of framework design: 3D FEA study. *J Prosthodont Res*. 2018;62:227–233.
33. Chang HC, Chang CH, Li HY, Wang CH. Biomechanical analysis of the press-fit effect in a conical Morse taper implant system by using an in vitro experimental test and finite element analysis. *J Prosthet Dent*. 2022;127:601–608.
34. Shams A, Elsherbini M, Elsherbiny AA, Özcan M, Sakrana AA. Rehabilitation of severely-destructed endodontically treated premolar teeth with novel endocrown system: Biomechanical behavior assessment through 3D finite element and in vitro analyses. *J Mech Behav Biomed Mater*. 2022;126:105–113.
35. Carneiro Pereira AL, Bezerra De Medeiros AK, De Sousa Santos KÉ, Barbosa GAS, Carreiro ADaFP. Accuracy of CAD-CAM systems for removable partial denture framework fabrication: A systematic review. *J Prosthet Dent*. 2021;125:241–248.
36. Penteado MM, Tribst JPM, Jurema ALB, Saavedra GSFA, Borges ALS. Influence of resin cement rigidity on the stress distribution of resin-bonded fixed partial dentures. *Comput Methods Biomech Biomed Engin*. 2019;22:953–960.

37. Shinya A, Yokoyama D, Lassila LV, Shinya A, Vallittu PK. Three-dimensional finite element analysis of metal and FRC adhesive fixed dental prostheses. *J Adhes Dent.* 2008;10:365–371.
38. Sukumoda E, Nemoto R, Nozaki K, et al. Increased stress concentration in prosthesis, adhesive cement, and periodontal tissue with zirconia RBFDPs by the reduced alveolar bone height. *J Prosthodont.* 2021;30:617–624.
39. Abe Y, Nogami K, Mizumachi W, Tsuka H, Hiasa K. Occlusal-supporting ability of individual maxillary and mandibular teeth. *J Oral Rehabil.* 2012;39:923–930.
40. Wang Y-L, Cheng J, Chen Y-M, Yip KH-K, Smales RJ, Yin X-M. Patterns and forces of occlusal contacts during lateral excursions recorded by the T-Scan II system in young Chinese adults with normal occlusions. *J Oral Rehabil.* 2011;38:571–578.
41. Gonzalez Y, Iwasaki LR, McCall Jr WD, Ohrbach R, Lozier E, Nickel JC. Reliability of electromyographic activity vs. bite-force from human masticatory muscles. *Eur J Oral Sci.* 2011;119:219–224.
42. Manns A, Rojas V, Van Diest N, Rojas D, Sampaio CS. Comparative study of molar and incisor bite forces regarding deciduous, mixed, and definitive dentition. *Cranio.* 2022;40:373–380.
43. Al-Wahadni A, Dkmak MSF, Almohammed S, Hatamleh MM, Tabanjah A. Fracture strength of anterior cantilever resin-bonded fixed partial dentures fabricated from high translucency zirconia with different intaglio surface treatments. *J Prosthodont.* 2024;33:358–366.
44. Quigley NP, Loo DSS, Choy C, Ha WN. Clinical efficacy of methods for bonding to zirconia: A systematic review. *J Prosthet Dent.* 2021;125:231–240.

Corresponding author:
Dr Yuhua Wang
Department of Prosthodontics
Shanghai Ninth People's Hospital
Shanghai Jiao Tong University School of Medicine
College of Stomatology
Shanghai Jiao Tong University
National Center for Stomatology
National Clinical Research Center for Oral Diseases
Shanghai Key Laboratory of Stomatology
Shanghai Research Institute of Stomatology
No. 639, Zhizaoju Road
Huangpu District, Shanghai 200011
PR CHINA
Email: wangyh1707@sh9hospital.org.cn

CRediT authorship contribution statement

Yujia Liu: Conceptualization, Methodology, Writing - original draft, Writing-review and editing. **Yijia Huang**: Software, Writing - original draft. **Sijing Chu**: Software. **Qiangqiang Fu**: Formal analysis. **Haixia Liu**: Funding acquisition. **Fan He**: Validation. **Yuhua Wang**: Supervision, Resources, Project administration.

https://doi.org/10.1016/j.prosdent.2025.01.035